Quaternary Research 77 (2012) 159–170

Contents lists available at SciVerse ScienceDirect

Quaternary Research

journal homepage: www.elsevier.com/locate/yqres

Variability of Indian monsoonal rainfall over the past 100 ka and its implication for C_3–C_4 vegetational change

Shailesh Agrawal [a,*], Prasanta Sanyal [b], Anindya Sarkar [a], Manoj Kumar Jaiswal [b], Koushik Dutta [c]

[a] Department of Geology and Geophysics, Indian Institute of Technology, Kharagpur, 721302, India
[b] Department of Earth Sciences, Indian Institute of Science Education and Research, Kolkata, 741252, India
[c] Large Lakes Observatory, University of Minnesota, Duluth, Duluth, MN 55812, USA

ARTICLE INFO

Article history:
Received 1 March 2011
Available online 19 October 2011

Keywords:
South-central Ganga Plain
Monsoonal rainfall
C_3–C_4 plants
Late Quaternary deposit
Soil carbonate
Optical dating

ABSTRACT

Oxygen and carbon isotope ratios of soil carbonate and carbon isotope ratios of soil organic matter (SOM) separated from three cores, Kalpi, IITK and Firozpur, of the Ganga Plain, India are used to reconstruct past rainfall variations and their effect on ambient vegetation. The $\delta^{18}O$ values of soil carbonate ($\delta^{18}O_{SC}$) analyzed from the cores range from −8.2 to −4.1‰. Using these variations in $\delta^{18}O_{SC}$ values we are able, for the first time, to show periodic change in rainfall amount between 100 and 18 ka with three peaks of higher monsoon at about 100, 40 and 25 ka. The estimation of rainfall variations using $\delta^{18}O$ value of rainwater-amount effect suggests maximum decrease in rainfall intensity (~20%) during the last glacial maximum. The $\delta^{13}C$ values of soil carbonate ($\delta^{13}C_{SC}$) and SOM ($\delta^{13}C_{SOM}$) range from −6.3 to +1.6‰ and −28.9 to −19.4‰, respectively, implying varying proportions of C_3 and C_4 vegetations over the Ganga Plain during the last 100 ka. The comparison between monsoonal rainfall and atmospheric CO_2 with vegetation for the time period 84 to 18 ka indicate that relative abundances of C_3 and C_4 vegetations were mainly driven by variations in monsoonal rainfall.

Introduction

During the Quaternary Period, global climate has oscillated between glacial and interglacial conditions (Cane, 1998; Clement et al., 1999) and the Indian monsoon has responded to these climatic changes (Prell and Van Campo, 1986; Prell and Kutzbach, 1987). Past monsoon reconstructions from marine sediments suggest that the glacial and interglacial periods were characterized by weaker and stronger summer monsoons, respectively (Prell and Van Campo, 1986; Clemens and Prell, 1990; Clemens et al., 1991). Model simulations suggest that the Indian summer monsoon rainfall varied by up to 30% during the last 150 ka as a result of changes in insolation coupled with glacial–interglacial conditions (Prell and Kutzbach, 1987). Most of these studies used proxy records that respond to wind-induced upwelling, and therefore essentially relate to the variation in wind speeds. However, rainfall associated with Indian summer monsoon depends on the moisture content and transportation path of wind rather than the speed (Clemens et al., 1996; Sarkar et al., 2000). There have been several attempts to reconstruct the past monsoon from continental records (Wasson et al., 1983; Tandon et al., 1997; Juyal et al., 2000, 2006, 2009; Gibling et al., 2005). However, the inferences made from those studies are qualitative in nature, and no quantitative estimate on the amount of monsoon rainfall variability for the late Quaternary (last 0.5 Ma) is available.

The alluvial sediments of the Ganga Plain, which lie in the path of the Indian summer monsoon, provide an excellent archive for past rainfall reconstructions. The sediments in the Ganga Plain are mainly deposited by perennial and monsoon-fed rivers (Ganga, Yamuna, Chambal etc.; Fig. 1). Gibling et al. (2005) proposed that variations in monsoonal rainfall affect the river system in the Ganga Plain. However, in absence of rainfall variation data, the climate forcing on the river system remains speculative. The presence of soil carbonates in the Ganga Plain sediments, whose isotopic composition is controlled by rainwater due to isotopic exchange, are useful in reconstruction of the temporal changes in rainfall amount.

The nature and types of vegetation are governed by ambient atmospheric CO_2 concentrations and rainfall amounts (Ehleringer, 2005; Osborne and Beerling, 2006). For example, it has been suggested that C_4 plants, which can more efficiently assimilate CO_2, evolved in response to the lowering of atmospheric CO_2 during the late Miocene (Cerling et al., 1997). On the other hand, the high water-use efficiency of C_4 plants suggests a strong dependency on temperature and seasonal rainfall (monsoon) in their emergence and proliferation (Pagani et al., 1999; Sanyal et al., 2004, 2005, 2010). The factors responsible for spatial and temporal variations of C_3 and C_4 plants abundances, however, are still a subject of considerable debate.

The present study aims to reconstruct the monsoon rainfall variations and vegetation history of the Ganga Plain for the last ~100 ka

* Corresponding author at: Research Scholar, Department of Geology and Geophysics, Indian Institute of Technology, Kharagpur, WB, 721 302, India. Fax: +91 322 228 2268.
E-mail address: as.shail@gmail.com (S. Agrawal).

0033-5894/$ – see front matter © 2011 University of Washington. Published by Elsevier Inc. All rights reserved.
doi:10.1016/j.yqres.2011.09.003

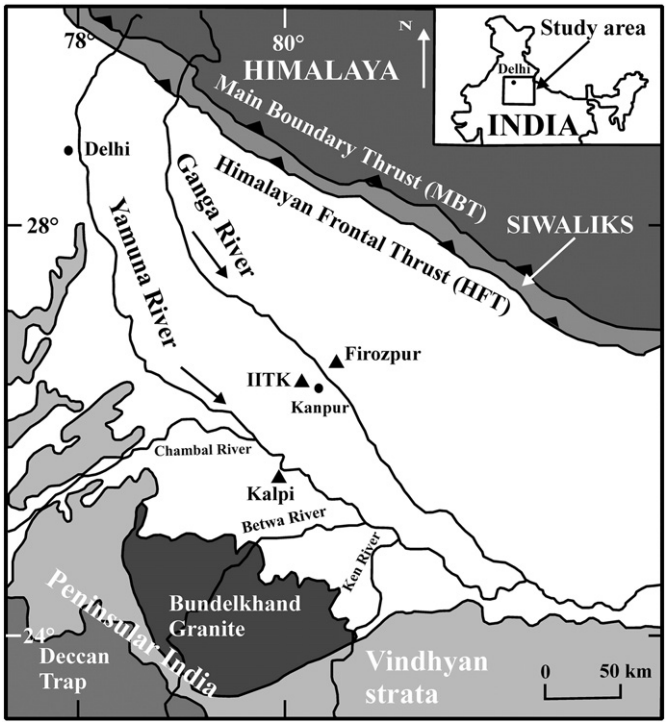

Figure 1. Map (after Gibling et al., 2005) showing locations of the Kalpi, IITK and Firozpur cores (solid triangles). The Kalpi core was drilled from the southern bank of the Yamuna River; the IITK core was taken from the interfluve area of the Ganga–Yamuna River; the Firozpur core was taken from the valley-fill deposits of the Ganga River.

using oxygen ($\delta^{18}O_{SC}$) and carbon isotope ratios ($\delta^{13}C_{SC}$) of soil carbonate and carbon isotope ratios of coexisting organic matter ($\delta^{13}C_{SOM}$). By comparing the rainfall data and available pCO_2 records (Barnola et al., 1987) with abundances of C_3 and C_4 plants, we attempt to ascertain the forcing factors (rainfall and pCO_2) in the relative abundance of C_4 plants during the late Quaternary.

Study area

The Ganga Plain covers an area of ~250,000 km^2 between 77°E to 88°E longitude and 24°N to 30°N latitude. It lies between the northern Himalayan foothills (Siwalik) and the southern Peninsular India (Fig. 1), and made of sediments derived from the Himalaya and the Peninsular India. The study area lies within the south-central part of the Ganga Plain (Fig. 1) where the late Quaternary sequences are exposed along incised valley of major rivers. The rainfall observed here is on average 800–1000 mm/yr, and the mean maximum and minimum temperatures range are 30–32°C and 15–18°C, respectively (Singh, 1994).

Three sediment cores, Kalpi (50 m), IITK (50 m) and Firozpur (25 m), were drilled for this study and are described as follows:

Kalpi core

The Kalpi core (Fig. 2a) was drilled from the top part of a cliff section at Kalpi, along the Yamuna River ("Kalpi cliff"). The sediments in the Kalpi core are alternating floodplain and sand deposits (Fig. 2a). Rhizoconcretions, mottles and Fe/Mn nodules, which indicate pedogenic activity during the pauses in sedimentation, are found within the floodplain and channel deposits. Thick accumulations of carbonates are observed at depths of ~22 and 30 m. These carbonates are comparable with the ground-water calcrete of the Kalpi cliff section (Sinha et al., 2006). The details of the dating technique used on the Kalpi core samples are provided in methodology section below.

IITK core

The IITK core (Fig. 3a) belongs to interfluve region of the Ganga Plain and contains mainly fine-grained floodplain sediments interspersed with minor sand layers (Sinha et al., 2007). Except in some parts of the IITK core, the presence of thick soil layer, dark mottles and rhizoconcretions indicates that the floodplain units have undergone pedogenesis (Sinha et al., 2007). The floodplain units of the IITK core yield strong magnetic signatures which also suggest pedogenesis (Sangode and Bloemendal, 2005; Sinha et al., 2007). A thick accumulation of carbonate is observed at a depth of ~14 m. Four Optically Stimulated Luminescence (OSL) ages 30.3 ± 3.4, 38.7 ± 3.7, 63 ± 4.0 and 86 ± 7.4 ka have been obtained for IITK core at 11.6, 21.5, 31.86 and 41.93 m depths, respectively (Sinha et al., 2007).

Firozpur core

The Firozpur core (Fig. 4a) was obtained from a valley-fill deposit of the Ganga Plain at Firozpur. The core is marked by alternate channel and floodplain facies with two fining-upward cycles. Sinha et al. (2007) interpreted this observation as repeated events of valley aggradation. Floodplain facies of the Firozpur core (10–20 m depth) is characterized by abundance of carbonate nodules and black mottles, which indicate that floodplain units have undergone pedogenesis. The lower floodplain and channel unit contain a thick accumulation of carbonates. Three OSL ages have been obtained for the Firozpur core at 4.6, 7.6 and 18.5 m which correspond to 8.5 ± 1.2, 10.5 ± 1.7 and >31.6 ± 2.7 ka respectively (Sinha et al., 2007).

Most paleosols in the Ganga Plain are accretionary (Sinha et al., 2007) implying that nodules at the bottom of paleosol unit are the oldest and those at the top of profile are the youngest. Isotopic ratios of soil carbonate nodules, therefore, record continuous time-series rather than time-averaged states.

Sample description

The diameter of carbonate nodules collected from the cores ranges from 0.5 to 5 cm (Figs. 5a,b). On the basis of megascopic property (size and form), host sediment (sand or mud), degree of indurations and petrographic characters, carbonates of the Ganga Plain have been classified as pedogenic (soil carbonates) and non-pedogenic carbonate (ground-water) (Sinha et al., 2006). Soil carbonates are common in all the three cores, except in part of the IITK core. Each nodule was divided into two halves. One-half was used for making a thin section for microscopic studies and the remaining half was used for isotopic analyses of carbonates. The thin sections of the soil carbonate from the Kalpi, IITK and Firozpur cores (Figs. 5a1,a2,a3) reveal that the calcium carbonate is mostly micritic in nature. Small amounts of sparry calcite (Figs. 5a2) indicate that there has been insignificant recrystallization of micrite since the initial precipitation of the carbonates. Thin sections of groundwater carbonates from the channel unit of the Kalpi and Firozpur cores show abundant floating grains (mainly quartz and small amounts of muscovite and biotite) in a sparry groundmass (Figs. 5b1,c1). The carbonates in muddy sediments from the lower part of the Firozpur core are also micritic and occur with an accumulation of quartz grains (Fig. 5d1).

Methodology

Optical dating of the Kalpi core sediments

Luminescence dating techniques rely on the principle that the luminescence response of naturally occurring minerals to environmental

https://doi.org/10.1016/j.yqres.2011.09.003 Published online by Cambridge University Press

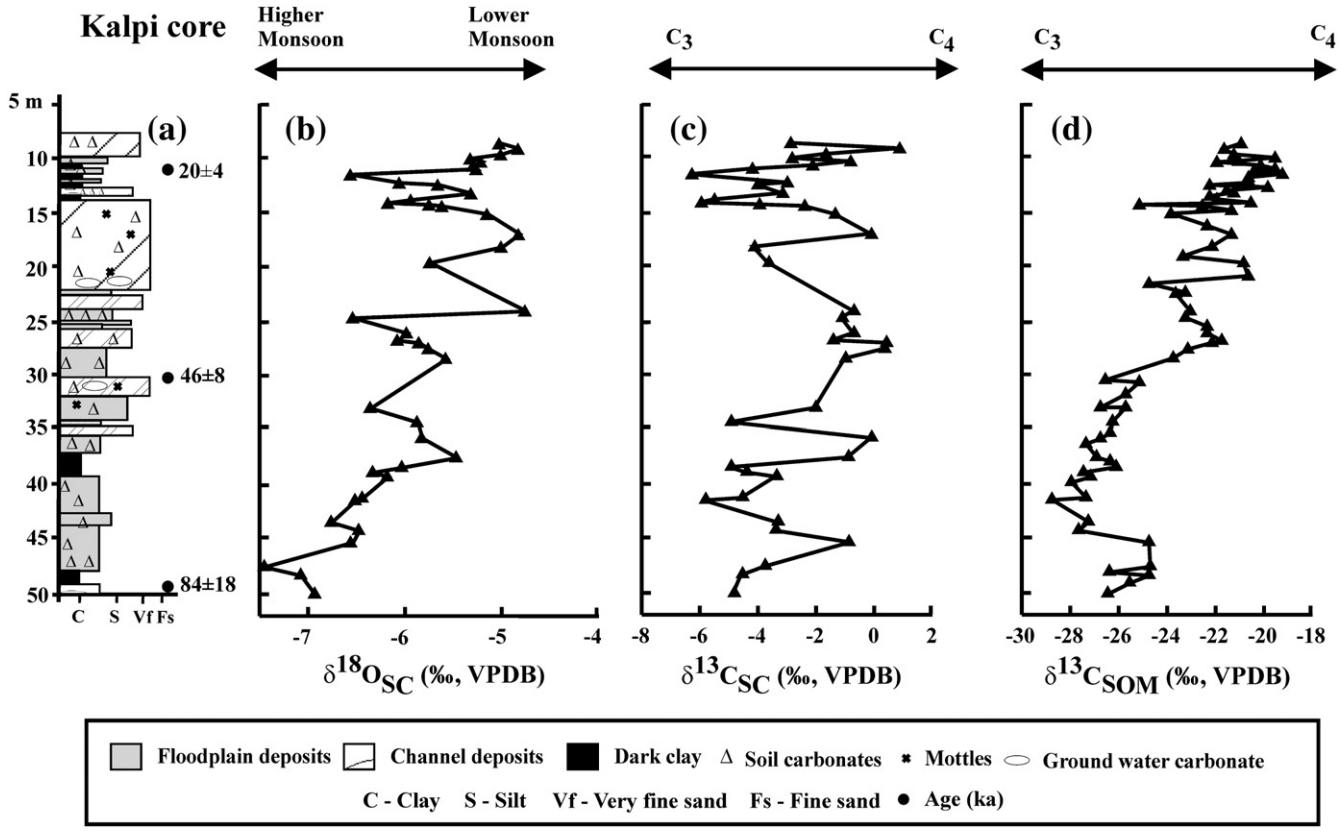

Figure 2. (a) Litholog of the Kalpi core collected from the Ganga Plain and variations in: (b) $\delta^{18}O_{SC}$, (c) $\delta^{13}C_{SC}$, and (d) $\delta^{13}C_{SOM}$ with respect to depth. The $\delta^{18}O_{SC}$ values show shorter term isotopically negative intervals at 50, 25 and 14 m depth (b). These negative intervals of $\delta^{18}O_{SC}$ values represent high monsoon conditions and correspond to 84, 40 and 25 ka, respectively. The $\delta^{13}C_{SC}$ values show negative intervals around 50, 35 and 14 m depth (c), almost coinciding with high monsoon intervals. The $\delta^{13}C_{SC}$ values show mixed C_3–C_4 vegetation with higher abundance of C_3 plants during high monsoon. The $\delta^{13}C_{SOM}$ values show negative intervals from 50 to 30 m depth (d), indicating higher abundance of C_3 plants.

radiation is cumulative over time and during transportation of sediment, geological luminescence (trapped charges) is reduced to a residual level by exposure of the sediment to sunlight (bleaching). Once sediment is buried, accumulation of luminescence occurs due to ionizing radiation arising from ambient radioactivity from U, Th and K. Hence, the luminescence concentration in the mineral is a function of burial time and the intensity of radioactivity in the sample environment (Aitken, 1998).

Core samples for optical dating were collected and sequentially pretreated for removing carbonate and organic carbon with 10% HCl and 30% H_2O_2, and 90–150 μm size fractions were obtained by dry sieving. The pure quartz fractions were eventually extracted via density separation with sodium polytungstate ($\rho = 2.58$ g/cm^3). Quartz grains thus obtained were treated with 40% HF for 80 min to remove alpha-affected layers and to remove feldspar contamination, if present. After etching, sample KP-4 did not yield enough quartz for analysis. Samples KP-5 and KP-6 showed early saturation; hence, the feldspar extracted from these two samples was analyzed using Infra-Red Stimulated Luminescence (IRSL) dating with the Single Aliquot Regeneration (SAR) protocol (Murray and Wintle, 2003). Considering that feldspars are prone to loss of luminescence signal at room temperature, 'fading' corrections suggested by Huntley and Lamothe (2001) and Auclair et al. (2003) were applied to obtain fading-corrected ages. In order to estimate the environmental dose rates, XRF and ICP-MS were used to measure the concentrations of U, Th and K in the sediment samples.

In view of the saturation effect on quartz, an attempt was made to use an evolving technique called the Iso-thermal luminescence (ITL) (Jain et al., 2005) on the quartz extracted from samples KP-5 and KP-6. However, the ITL ages were significantly overestimated (~40% residual luminescence after bleaching for 1000 s). Therefore, fading-corrected IRSL ages obtained on feldspar were used as the best estimates for ages of the Kalpi core samples.

In order to check the reliability of the IRSL-SAR protocol used on the feldspar minerals, standard tests were performed: preheat plateau, thermal transfer, dose recovery, etc. (Murray and Wintle, 2000). The results indicate that the samples can be analyzed by the standard SAR protocol of Murray and Wintle (2000). The dating of the samples was done at the Department of Geosciences, National Taiwan University, Taipei, Taiwan.

Isotopic analysis of carbonates

Samples for isotopic analyses were taken from the fresh surface of the nodules by a dental drill under microscope to avoid sampling of fracture-fill carbonates. Powdered samples were reacted with 100% H_3PO_4 at 72°C in the Gas Bench II coupled with Finnigan Delta^{Plus}XP Continuous Flow Isotope Ratio Mass Spectrometer (CFIRMS). The C and O isotope ratios were measured from the evolved CO_2 in a CFIRMS. Long-term (~1 yr) measurements of in-house $CaCO_3$ standards BDH (procured from University College London) and Z-Carrara (procured from Physical Research Laboratory, Ahmedabad) that were calibrated via NBS-19 provide an external precision of ±0.1‰ (2σ) for both the $\delta^{18}O$ and $\delta^{13}C$ values.

Isotopic analysis of soil organic matter (SOM) and modern plant samples

The individual paleosol samples were powdered and thereafter decarbonated using 0.5 N HCl. Acid and soluble salts were removed by centrifuging (~3000 rpm) with deionized water. Subsequently,

https://doi.org/10.1016/j.yqres.2011.09.003 Published online by Cambridge University Press

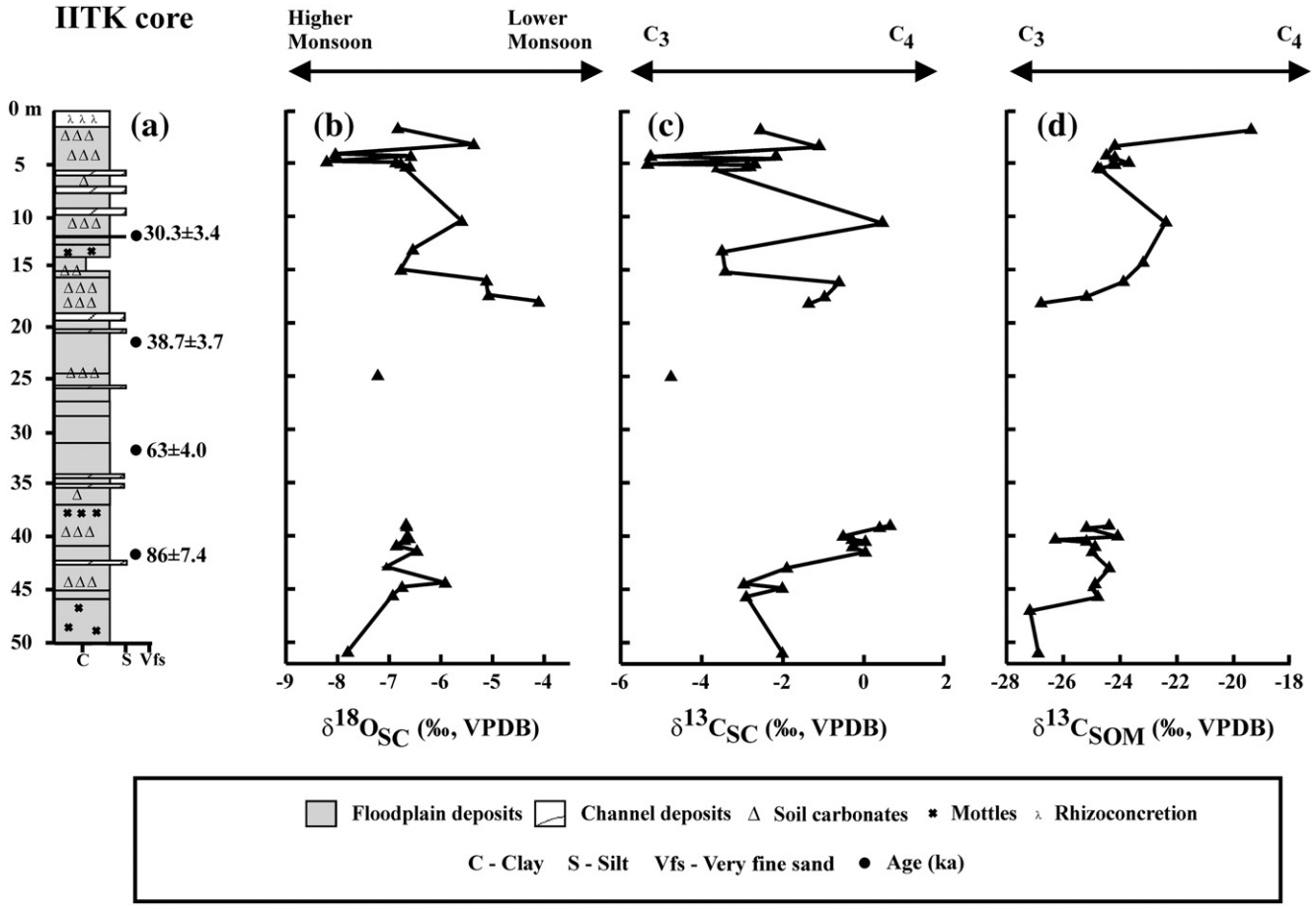

Figure 3. (a) Litholog of the IITK core (Sinha et al., 2007) collected from the Ganga Plain and variation in (b) $\delta^{18}O_{SC}$, (c) $\delta^{13}C_{SC}$ and (d) $\delta^{13}C_{SOM}$ values with respect to depth. The (b) $\delta^{18}O_{SC}$ values show isotopically negative intervals around 50 and 5 m depth, which suggest high monsoon phases around 100 and 22 ka. The (c) $\delta^{13}C_{SC}$ and (d) $\delta^{13}C_{SOM}$ values show negative intervals around 50 and 5 m that suggest higher abundance of C_3 plants.

the decarbonated samples were dried in an oven at 70°C. The dried samples were crushed to make a fine powder.

To analyze $\delta^{13}C$ values of modern C_3 and C_4 plants, grass samples were collected from the south-central part of the Ganga Plain (Bithur and the Kalpi cliffs) and the Kharagpur region. The plant samples were washed with dilute HCl, rinsed with water and oven dried and then crushed to make fine powder. 10–25 mg of the powdered sample of SOM and ~100 μg samples of modern plants were combusted in a Flash EA 1112 elemental analyzer coupled with CFIRMS. The IAEA standard C-3 Cellulose was analyzed along with each set of samples, to calibrate the data and check the reproducibility. Both C-3 and UBC-ACE (Acetanilide) were used to monitor analytical precisions. All isotopic data are reported against VPDB with a routine precision of ±0.1‰ (2σ) for $\delta^{13}C$ values. All carbonates, organic matter and plant samples were analyzed in the Stable Isotope Laboratory National facility of the Indian Institute of Technology, Kharagpur, India.

Results

Ages of the Kalpi core

Three ages were obtained from the Kalpi core at depths 10.33 m, 30.6 m and 50.24 m. These ages are 20 ± 4 ka (KP-4), 46 ± 8 ka (KP-5) and 84 ± 18 ka (KP-6), respectively (Fig. 2a; Table 1).

$\delta^{13}C$ values of modern plants

The $\delta^{13}C$ values of C_3 plants from south-central part of the Ganga Plain and the Kharagpur region range from −32.6 to −19.2‰ and average −29.5 ± 2.2‰ (n = 47) (Table S1) and for C_4 plants the value range from −16.6 to −10.5‰ and average −13.0 ± 1.4‰ (n = 35) (Table S2).

$\delta^{18}O$ and $\delta^{13}C$ values in soil carbonate and $\delta^{13}C$ values in SOM

Intra-profile isotopic variability

Figure 6 shows intra-profile variation of $\delta^{18}O_{SC}$ and $\delta^{13}C_{SC}$, both lateral and vertical where samples were available, in the four profiles of the Kalpi core. The $\delta^{18}O_{SC}$ values are more or less constant in both directions (lateral and vertical) for profiles 1, 2 and 3 (Figs. 6a,b,c). In case of profile 4, the $\delta^{18}O_{SC}$ values show very little enrichment toward the top (Fig. 6d). The $\delta^{13}C_{SC}$ values do not show continuous enrichment or depletion with depth except for profile 4 where enrichment is observed (Fig. 6d).

Kalpi core

The $\delta^{18}O_{SC}$ values in the Kalpi core range from −7.5 to −4.8‰ (Table S3). The variations of oxygen isotope ratio show enrichment in ^{18}O from bottom to top part of the core (Fig. 2b) with distinct fluctuation. Overall, the $\delta^{18}O_{SC}$ values show more negative intervals at ~50, 25 and 12 m and less negative intervals at ~37, 17 and 8 m depth (Fig. 2b).

The $\delta^{13}C_{SC}$ values in the Kalpi core samples range from −6.3 to +0.9‰ (Table S3). The $\delta^{13}C_{SC}$ values show more negative intervals at ~10 m and between 50 and 30 m depth. Less negative intervals were measured at ~35, 27 and 8 m (Fig. 2c).

The $\delta^{13}C_{SOM}$ value in the Kalpi core samples range from −28.9 to −19.4‰ (Table S3). From 50 to 30 m, the $\delta^{13}C_{SOM}$ values remain

https://doi.org/10.1016/j.yqres.2011.09.003 Published online by Cambridge University Press

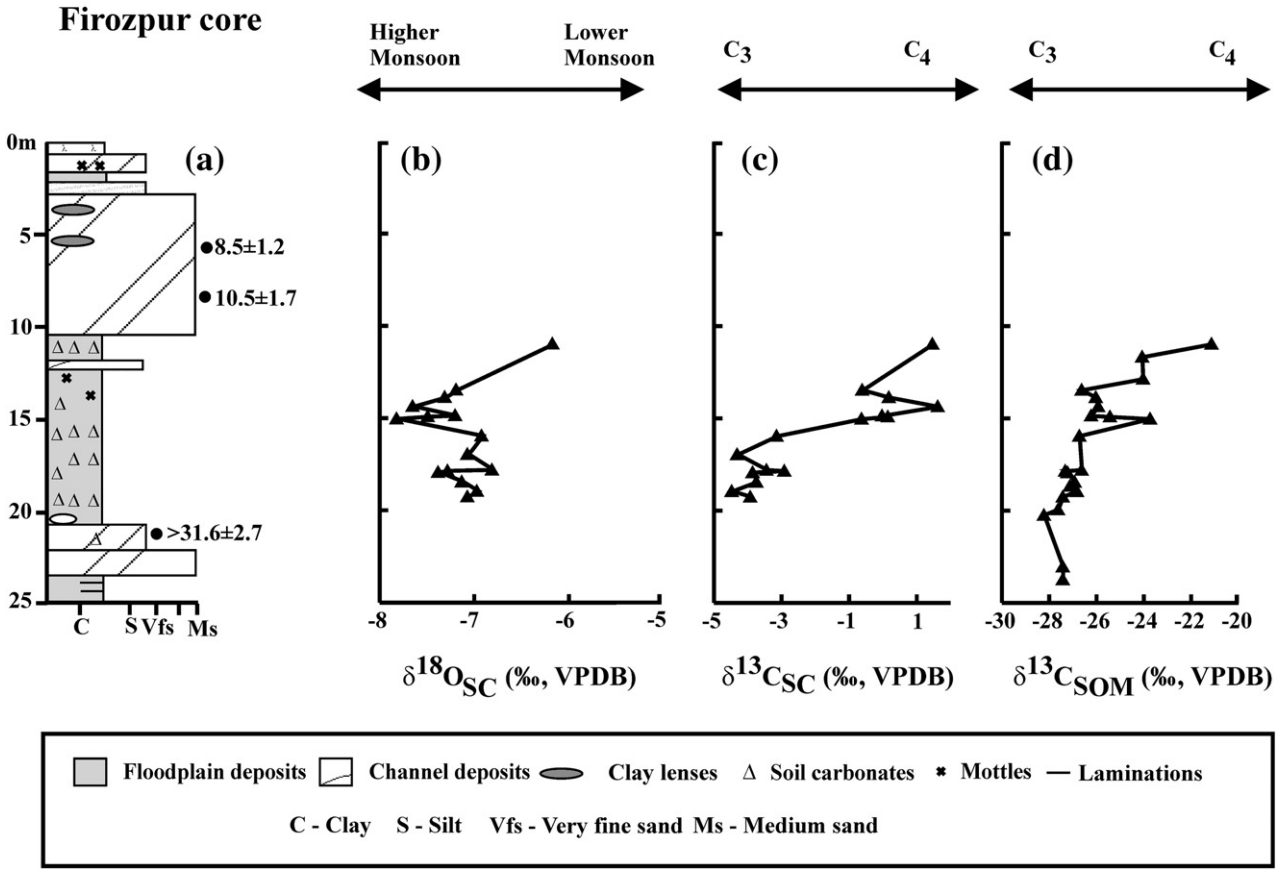

Figure 4. (a) Litholog of the Firozpur core (Sinha et al., 2007) collected from the Ganga Plain and variation in (b) $\delta^{18}O_{SC}$, (c) $\delta^{13}C_{SC}$ and (d) $\delta^{13}C_{SOM}$ values with respect to depth. The $\delta^{18}O_{SC}$ values show short term isotopically negative interval around 15 m (b) and represent high monsoon conditions. (c) The $\delta^{13}C_{SC}$ and (d) $\delta^{13}C_{SOM}$ values show overall enrichment from 20 to 11 m which suggests a decrease in C_3 abundance from 30 to 18 ka.

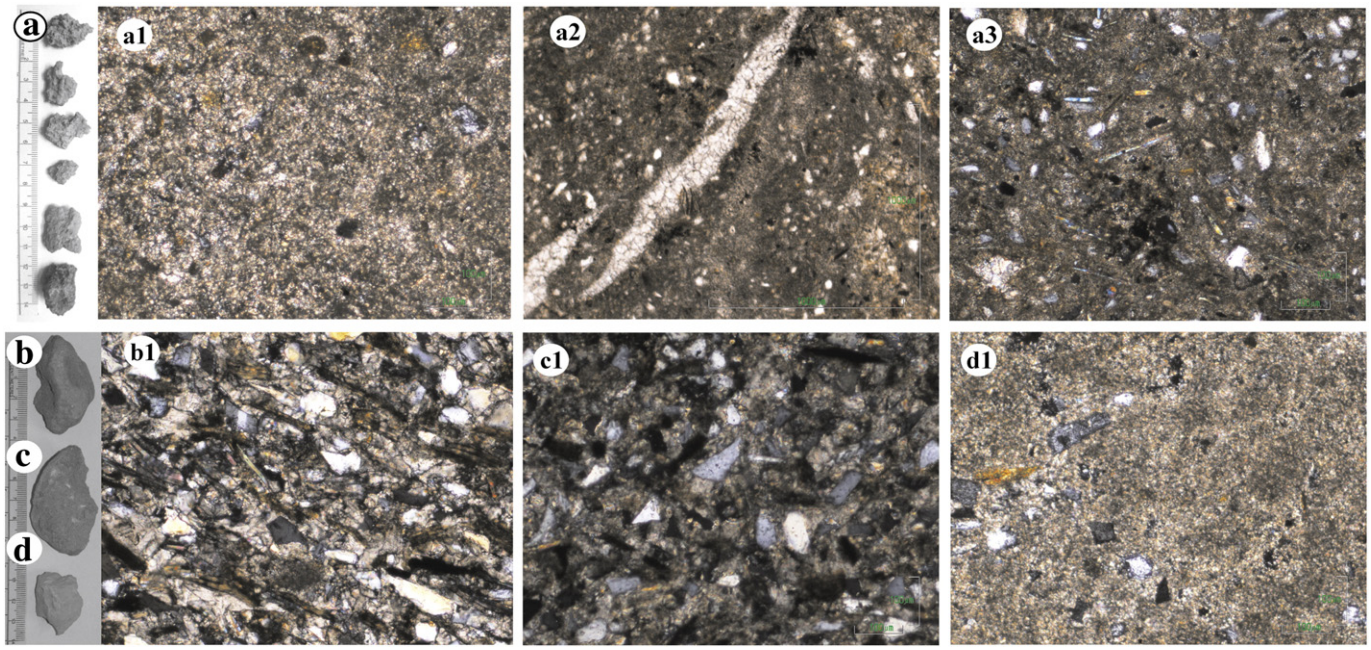

Figure 5. (a) Soil-carbonate nodules from the Kalpi, IITK and Firozpur cores. Photomicrograph of soil-carbonate nodules from the Kalpi (a1), IITK (a2) and Firozpur cores (a3) displaying mostly micritic nature. Presence of small amount of sparry calcite indicates that no major recrystallization has taken place after precipitation of carbonates (a2). Groundwater carbonates from channel sand of (b) Kalpi and (c) Firozpur cores, and floodplain sediments of (d) Firozpur core. Photomicrograph of ground-water carbonates from the channel unit shows abundant floating grains (mainly quartz and small amount of muscovite and biotite) in a spar groundmass (b1, c1). Also, photomicrograph of the carbonates from the muddy layer of the lower part of the Firozpur core shows floating grains of quartz (d1) in micritic groundmass.

https://doi.org/10.1016/j.yqres.2011.09.003 Published online by Cambridge University Press

Table 1
Luminescence chronology of the Kalpi core.

Samples	Depth (m)	Radioactive element concentration			Dose rate (Gy/ka)	Paleodose (uncorrected) (Gy)	Average 'g' values	Ages (corrected) (ka)
		U (ppm)	Th (ppm)	K (%)				
KP-4	10.25–10.40	2.29 ± 0.02	12.58 ± 0.09	2.13	3.48 ± 0.3	41.1 ± 4.4	5.0	20 ± 4
KP-5	30.52–30.68	3.41 ± 0.02	18.58 ± 0.1	1.90	3.98 ± 0.4	115.7 ± 10.6	4.5	46 ± 8
KP-6	50.20–50.28	1.90 ± 0.02	13.65 ± 0.07	3.55	4.48 ± 0.4	196.4 ± 15.2	5.7	84 ± 18

between −28.9 and −24.9‰ (Fig. 2d). The 30 m depth is characterized by a gradual increase in $\delta^{13}C_{SOM}$ values to −22‰ ~27 m. $\delta^{13}C_{SOM}$ values become less negative up to −21.1‰, ~8 m depth (Fig. 2d).

IITK core

The soil carbonate nodules are mostly found in the lower and upper parts of the core. A single nodule is found between 39 and 18 m (Fig. 3a). The $\delta^{18}O_{SC}$ values in the IITK core range from −8.2 to −4.1‰ (Table S3). Between 50 and 39 m depth, $\delta^{18}O_{SC}$ values record an overall trend toward less negative values from −7.8 to −5.9‰, (Fig. 3b). In the top part of the core, at about 18 m, a value of −4.1‰ is observed. Samples above 18 m are characterized by decrease in $\delta^{18}O_{SC}$ value up to 5 m (Fig. 3b). The most depleted phase occurred at 5 m which is followed by phase of enrichment up to 3 m (Fig. 3b).

The $\delta^{13}C_{SC}$ values range from −5.4 to +0.6‰ (Table S3). From 50 to 39 m $\delta^{13}C_{SC}$ values show gradual enrichment. In the top part of the core at about 13 and 5 m, minimum $\delta^{13}C_{SC}$ values are observed (Fig. 3c). On the other hand, less negative intervals are observed at depths of ~18, 10 and 3 m (Fig. 3c).

The $\delta^{13}C_{SOM}$ values range from −27.2 to −19.4‰ (Table S3), depicting a gradual enrichment in the sections from 50 to 39 m and from 18 to 13 m (Fig. 3d). The top 18 m is characterized by fluctuations in $\delta^{13}C$ values; the maximum enriched value is observed at ~3 m (Fig. 3d).

Firozpur core

The $\delta^{18}O_{SC}$ values in the Firozpur core range from −7.8 to −6.2‰ (Table S3). There is a trend towards more negative $\delta^{18}O_{SC}$ values from −6.8 to −7.8‰ between 20 and 15 m (Fig. 4b). This is followed by less negative $\delta^{18}O_{SC}$ trend between 15 and 11 m (Fig. 4b).

The $\delta^{13}C_{SC}$ values range from −4.5 to +1.6‰ (Table S3). The data indicate depleted $\delta^{13}C$ values between 20 and 16 m (Fig. 4c) followed by gradual enrichment at depths up to 11 m. The enrichment observed in the top part of the core is similar in nature compared to that of the Kalpi and IITK core data.

The $\delta^{13}C_{SOM}$ values range from −28.2 to −21.1‰ (Table S3) with enrichment in ^{13}C from bottom to top parts of the core (Fig. 4d).

$\delta^{18}O$ and $\delta^{13}C$ values in ground-water carbonate

The $\delta^{18}O$ values of ground-water carbonate of the Kalpi core range from −5.7 to −4.8‰ (Table S3) whereas $\delta^{13}C$ values range from −1.0 to 0.9‰. $\delta^{18}O$ and $\delta^{13}C$ values in one ground-water carbonate sample from the IITK core are −6.3‰ and 1.7‰, respectively. The $\delta^{18}O$ of ground-water carbonates of the Firozpur core at about 18.7 and 20 m depths are −7.1 and −6.9‰, and $\delta^{13}C$ values are −2.0 to −1.2‰, respectively. On the other hand, $\delta^{18}O$ and $\delta^{13}C$ values of carbonate from the muddy bed are −7.8 and −4.1‰, respectively. There is little apparent isotopic difference observed between soil carbonates and ground-water carbonates in all the three cores, consistent with observations of Sinha et al. (2006).

Discussion

$\delta^{18}O$ values of soil carbonate

Oxygen isotope ratios of soil carbonate depend on the temperature of carbonate precipitation and isotopic ratio of soil water, normally derived from local rainfall. During the last 100 ka, the climate was characterized by fluctuations in rainfall and temperature. The

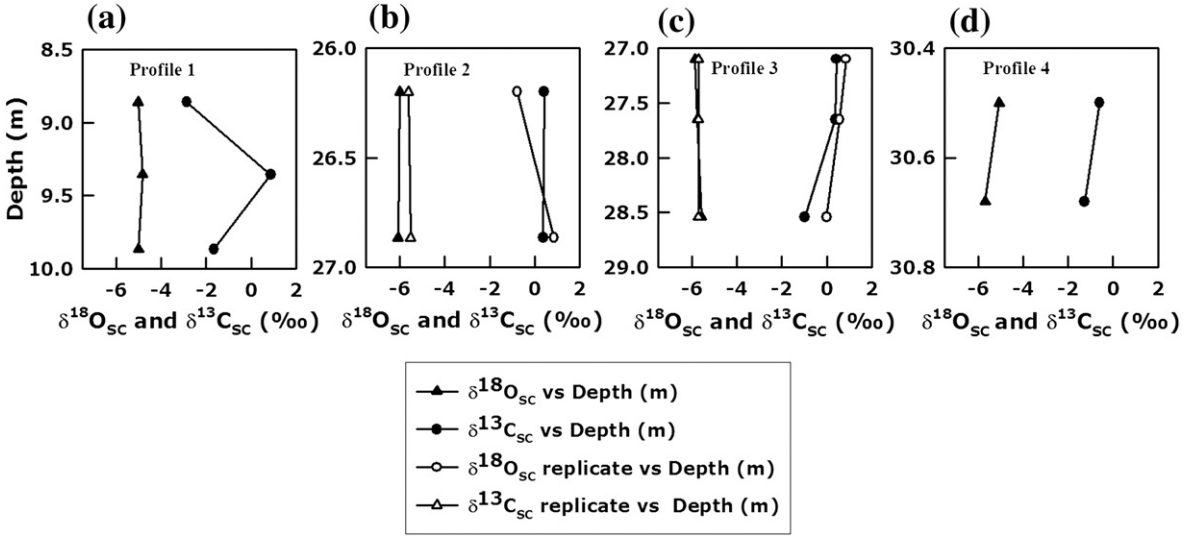

Figure 6. Intra-profile variations of oxygen and carbon isotope ratio in the Kalpi core. Near-constant $\delta^{18}O_{sc}$ value in a profile implies evaporation was not significant during the precipitation of soil carbonates. Replicate samples in a profile also show similar isotopic trends, supporting inference of insignificant evaporation. Carbon isotope ratio also shows almost similar pattern except in Profile 1 where higher variation is observed compared to oxygen isotope ratio.

https://doi.org/10.1016/j.yqres.2011.09.003 Published online by Cambridge University Press

$\delta^{18}O$ variability obtained from speleothem data suggests that during the last glacial maximum (LGM, ~18 ka), temperature in the tropical region was lowered by 3 to 4°C (Farrera et al., 1999). This temperature change can impart 0.8‰ variation in the $\delta^{18}O$ value of soil carbonate. As the observed variations in $\delta^{18}O_{SC}$ value of the Kalpi, IITK and Firozpur cores are more than 0.8‰, it can be inferred that the $\delta^{18}O_{SC}$ values in the Ganga Plain soil also recorded change in the $\delta^{18}O$ value of rainwater. However, due to evaporation near the surface, the $\delta^{18}O$ value of soil water is enriched in ^{18}O relative to the $\delta^{18}O$ values of rainwater, as ^{16}O is preferentially evaporated. The evaporation effect is most distinct in closed-basin lakes where water is lost by infiltration and evaporation (Talbot, 1990), as compared to soils. Soil carbonates form in seasonally dry environments, and during evaporation, soil water can be enriched by 1‰, as observed by Salomons et al. (1978) in western India. Very little enrichment in ^{18}O towards the top (Fig. 6d) together with near-constant $\delta^{18}O_{SC}$ values (Figs. 6a,b,c) in different profiles of the Kalpi core indicate that evaporation was not very significant there.

Considering the $\delta^{18}O$ value of modern soil water to be −5.4‰ (VSMOW) and mean annual temperature at Kanpur City, India, to be 25°C, the expected $\delta^{18}O$ value of soil carbonate is −7.3‰ (VPDB). This value is similar to the $\delta^{18}O$ value obtained for the younger soil carbonate (−7‰, VPDB) sample collected from the Ganga Plain (Sinha et al., 2006) implying that the $\delta^{18}O$ value of soil carbonate can be used to decipher paleo-precipitation in the Ganga Plain.

It has been observed in low-latitude sites that $\delta^{18}O$ value of rainwater decreases by 1.5‰ for every increase of 100 mm of rainfall (Yurtsever and Gat, 1981), a phenomenon commonly called the "amount effect" (Dansgaard, 1964). The $\delta^{18}O$ values of rainwater and rainfall data for the duration of 1961 to 2001 from the Delhi (Fig. 1) show lowering of the $\delta^{18}O$ value with an increase in amount of rain (Fig. S1; Bhattacharya et al., 2003), indicating that the amount effect can be applied to explain the variations in $\delta^{18}O$ values of soil carbonate. Hence, we interpret periods of more negative $\delta^{18}O_{SC}$ values as intervals of high rainfall and periods of less negative $\delta^{18}O_{SC}$ values as intervals of relatively low rainfall. Based on these assumptions, we discuss below an oxygen-isotope-based reconstruction of rainfall intensity of the southwest Indian monsoon over the past 100 ka.

The Kalpi core soil carbonate samples delineate three phases of distinct lowering in the $\delta^{18}O_{SC}$ values at about 50, 25 and 12 m (Fig. 2b), suggesting increases in monsoon rainfall intensities at ~84, 40 and 22 ka. Less negative $\delta^{18}O_{SC}$ values at depths of ~37, 17 and 8 m (60, 30 and 18 ka) indicate weaker monsoonal rainfall (Fig. 2b). Oxygen isotope data at ~50 and 5 m in the IITK core show high monsoonal rainfall during 100 and 22 ka, and low rainfall at ~80, 35 and 18 ka (Fig. 3b). The more negative $\delta^{18}O_{SC}$ interval in the Firozpur core at 15 m (~25 ka) suggests higher monsoon rainfall then relative to ~20 and 11 m depths (Fig. 4b). Overall, the age data of the Firozpur core suggests that the monsoonal rainfall has gradually increased from 30 to 25 ka. Subsequently, rainfall intensity decreased from 25 and 18 ka.

The Kalpi, IITK and Firozpur cores were collected from different parts of the Ganga Plain (Fig. 1). Nevertheless, the $\delta^{18}O_{SC}$ values record similar temporal trends. We interpret this synchronicity of oxygen isotope variations to indicate that during the last 100 ka, the Indian monsoon has undergone three periods of high monsoon rainfall intensities at ~100, 40, and 25 ka. The post 100 ka maximum intensity is followed by a gradual decrease in monsoon rainfall intensity until ~60 ka. Monsoon intensity maxima at 40 and 25 ka are followed by relative abrupt transitions to weaker monsoon intensity with weakest conditions at ~18 ka (LGM).

Using the relationship between the $\delta^{18}O$ value of rainwater and amount of rainfall (Yurtsever and Gat, 1981) and difference between the extreme $\delta^{18}O_{SC}$ values of individual enriched or depleted phases, changes in rainfall amount have been calculated for last 100 ka. Keeping the average rainfall amount to 1000 mm/year for Kanpur City, our results indicate that the rainfall amount during the last 100 ka had varied by 5 to 20% in the Ganga Plain. The maximum decrease of rainfall occurred between 25 and 18 ka (~200 mm decrease in rainfall), in agreement with the model data of Prell and Kutzbach (1987).

$\delta^{13}C$ values of soil carbonate and SOM

$\delta^{13}C$ values of soil carbonate and SOM can be used to reconstruct changes in vegetation across the landscape (Cerling, 1984; Cerling et al., 1989). Based on the photosynthetic pathway, terrestrial plants are divided into two groups, C_3 (Calvin cycle) and C_4 (Hatch–Slack cycle) plants. The $\delta^{13}C$ values of C_3 plants range from −34 to −19‰ and averages −26.7‰; whereas for C_4 plants it ranges from −18 to −10‰ and averages −12.5‰ (Cerling et al., 1997). The plant bio-organic residues are incorporated into the SOM after death of the plant. The SOM is assumed to preserve the mean carbon isotopic composition of the contemporary vegetation, with little or no fractionation. In contrast, soil carbonate forms from soil solution mixed with soil CO_2, derived from decomposition of SOM and plant respiration during a drying phase (Wang and Follmer, 1998). According to the Cerling (1984) diffusion-equilibrium model, $\delta^{13}C$ values of soil carbonate are enriched 14 to 17‰ (0 to 25°C) compared to the $\delta^{13}C$ values of SOM, provided the soil-derived CO_2 is high enough to overwhelm the contribution of CO_2 from the atmosphere in the soil. Considering the average $\delta^{13}C$ value of modern C_3 and C_4 plants from the Ganga Plain, it can be suggested that if the soil is characterized exclusively by C_3 plants, the expected $\delta^{13}C$ value of soil carbonate should be around −15.5‰. On the other hand, in case of C_4 plants, the $\delta^{13}C$ value of soil carbonate would be around +1.0‰. This would imply that periods of relatively low $\delta^{13}C$ values should correspond to high proportion of C_3 plants, while relatively high $\delta^{13}C$ values would indicate dominance of C_4 plants.

In the Kalpi core, $\delta^{13}C_{SC}$ values between 50 and 30 m depth (Fig. 2c) representing 84 to 45 ka, suggest mixed C_3–C_4 plants with 25–40% abundance of C_3 plants. On the other hand, $\delta^{13}C_{SOM}$ value indicates 70–95% abundance of C_3 plants between 84 and 45 ka (Fig. 2d). At ~27 m depth both $\delta^{13}C_{SC}$ and $\delta^{13}C_{SOM}$ values suggest higher abundance (~70–90%) of C_4 plants (Figs. 2c,d) corresponding to the 40 ka age of the core. Subsequently, $\delta^{13}C_{SC}$ values imply an increase to 60% in abundance of C_3 plants until 25 ka with fluctuations within this interval. This specific trend is not prominent in $\delta^{13}C_{SOM}$ but it shows gradual increase in $\delta^{13}C$ values from 21 to 15 m depth bracketed between 34 and 26 ka age of the core and suggests increasing abundance of C_3 plants (Fig. 2d). C_4 plants reached their peak at 18 ka, with 100% abundance (Fig. 2c).

The $\delta^{13}C_{SC}$ and $\delta^{13}C_{SOM}$ values from the IITK core show mixed C_3–C_4 vegetation with 20–25% and 70–80% abundance of C_3 plants at ~50 and 5 m (100 and 22 ka, respectively) (Figs. 3c,d). C_4 plants dominated at ~39, 18 and 3 m depth (80, 35 and 18 ka) with 85–100% abundance (Fig. 3c).

In the Firozpur core, $\delta^{13}C_{SC}$ values suggest 10–35% abundance of C_3 plants between 20 and 16 m depth (30 to 26 ka) whereas $\delta^{13}C_{SOM}$ suggests dominant C_3 vegetation (80–90%) between 30 and 26 ka (Figs. 4c,d). Subsequently, $\delta^{13}C_{SC}$ values show increasing abundance up to 75–100% of C_4 plants from 16 to 10 m (Fig. 4c) which is bracketed between 26 and 18 ka (LGM). On the other hand, $\delta^{13}C_{SOM}$ shows increasing abundance of C_4 plants up to 50% during the LGM (Fig. 4d).

The paleovegetation data obtained using $\delta^{13}C_{SC}$ and $\delta^{13}C_{SOM}$ values from the Kalpi, IITK and Firozpur cores suggest that the south-central Ganga Plain was characterized by mixed C_3–C_4 vegetation. Although trends of temporal change in vegetation obtained from $\delta^{13}C_{SC}$ and $\delta^{13}C_{SOM}$ are similar, estimates of C_3 or C_4 plants from these proxies differ. For example, at ~100 ka $\delta^{13}C_{SC}$ suggests 25% abundance of C_3 plants, whereas $\delta^{13}C_{SOM}$ indicates 85% C_3 plants. The probable causes for such mismatches are discussed below. After

https://doi.org/10.1016/j.yqres.2011.09.003 Published online by Cambridge University Press

100 ka, C_4 plants proliferated: by ~40 ka the C_3 component was reduced to ~10%. Similarly, the isotopic data suggest an overall increase in C_3 plants (up to 40%) that continued until ~25 ka. Subsequent to 25 ka there was rapid proliferation (90–100%) in C_4 plants, culminating during the LGM.

A higher percentage of C_4 plants is inferred from $\delta^{13}C$ values of soil carbonate than from SOM. The changes in the $\delta^{13}C$ values of soil CO_2 are related to the soil respiration rate and could affect the $\delta^{13}C$ values of soil carbonate. During arid conditions, the soil respiration rate decreases, allowing the entrance of atmospheric CO_2 to deeper levels in the soil profile and causing the positive shift in $\delta^{13}C$ values of soil carbonate. However, it is difficult to evaluate the importance of this effect in the geological past. On the basis of relationship between respiration rate and effective moisture, Andrews et al. (1998) assumed a high respiration rate in soil of the arid Thar Desert (average annual rainfall 300–400 mm) and suggested that atmospheric CO_2 had a negligible effect on the $\delta^{13}C$ values of soil carbonate there. It is reasonable to assume much higher respiration rate in the more humid south-central part of the Ganga Plain. Accordingly, we eliminate contribution of atmospheric CO_2 into soil CO_2 as a cause for the higher estimation of C_4 plants using the $\delta^{13}C$ value of soil carbonate.

Poor preservation of carbon in SOM can cause errors in the abundance of vegetation estimated from carbon isotopes. Studies on SOM degradation have indicated changes in $\delta^{13}C$ value by several per mil (Benner et al., 1987; Nadelhoffer and Fry, 1988; Wedin et al., 1995; Huang et al., 1996; Krull et al., 2002). Moreover, SOM derived from C_4 plants may be less resistant compared to the C_3 counterpart (Wynn and Bird, 2007) resulting in underestimation of abundances of C_4 plants. It is generally agreed that microorganisms degrade less resistant organic fractions of SOM like carbohydrates and proteins quickly compared to more resistant fractions such as lignin and lipids (Benner et al., 1987). Removal of these less resistant fractions gradually lowers the $\delta^{13}C$ values of SOM as carbohydrates and proteins more enriched than lignin and lipids in ^{12}C (Goni et al., 1997; Huang et al., 1999). Therefore, estimation of vegetation from such SOM would show erroneously high abundances of C_3 plants.

Correlation with other monsoon proxies

It is desirable to see whether the monsoonal rainfall variations reconstructed using oxygen isotope ratios of soil carbonate from the Ganga Plain are synchronous with other records. One potential difficulty in this exercise is dating error due to the different techniques used in each study. Our study generated OSL ages for the three cores from the Ganga Plain. The age model relating depth and time used an assumed constant sedimentation rate. The similar nature of isotopic trends in the top part of the cores suggests that this assumption was justified. Paleo-monsoon reconstruction based on the $\delta^{18}O$ values of soil carbonate from the continuous Kalpi core is compared with the marine oxygen isotope (MIS) and available terrestrial records below.

Correlation of monsoon with marine oxygen isotope stages

Monsoon wind strength and rainfall vary with glacial–interglacial climatic conditions (Prell and Kutzbach, 1987; Overpeck et al., 1996) which are commonly represented by the oxygen isotope ratios of foraminifera collected from deep-sea sediment core samples (Imbrie et al., 1984; Wright, 2000). Values of $\delta^{18}O$ in the foraminifera change as water from the oceans is temporarily stored as polar ice during glaciations. Patterns of change in the $\delta^{18}O$ record are summarized as marine oxygen isotope stages (MIS).

A comparison of MIS and paleoclimatic records from the Indian Ocean shows that the monsoon during MIS 3 (57–25 ka) was weaker than during both interglacial MIS 5 (128–75 ka) and MIS 1 (10–0 ka), but slightly stronger than during glacial MIS 4 (75–57 ka) and much stronger than during MIS 2 (25–10 ka) (Feng et al., 2007). Overall, there was a gradual decrease in monsoon strength from MIS 5 to MIS 2, punctuated by short-term fluctuations.

The $\delta^{18}O$ data from the Ganga Plain also correlates well with the marine record (Figs. 7b,c). The oldest sample in the Kalpi core is around 84 ka, in MIS 5. The data show higher monsoonal rainfall during 84 ka followed by gradually decreasing intensity with distinct fluctuations, similar to the pattern of $\delta^{18}O$ changes in the marine record. Monsoon strength was higher during MIS 5 than MIS 3, as is evident from the lower $\delta^{18}O_{SC}$ values during MIS 5. The post 40 ka data show a lowering of $\delta^{18}O_{SC}$ values, indicating the increase in monsoonal rainfall intensity that was characteristic of MIS 3. After 25 ka, the data depict an abrupt increase in $\delta^{18}O_{SC}$, consistent with the onset of the LGM (Figs. 7b,c). Again, this is similar to the pattern in the marine record.

Correlation of monsoon rainfall with terrestrial records

Reconstruction of the Indian monsoon based on variations in pollen, magnetic susceptibility and geochemical data have been done by various workers (Table S4; Figs. 7a,d). These records encompass a short period. Magnetic susceptibility and geochemical data of the Goting Lake sediments from the higher central Himalayas indicate moderate to strong monsoon circulation during 25 ka, whereas at ~22 ka the early LGM climate was mainly arid (Fig. 7d; Juyal et al., 2009). Bookhagen et al. (2005) showed a five-fold increase in erosion of the Sutlej Valley, Greater Himalaya, attributed to the strong monsoon during the late Pleistocene (29 to 24 ka; Fig. 7d). Stable isotope records of calcrete from the Thar Desert suggest weak monsoon intensities during MIS 4 and MIS 2 and strong monsoon during MIS 3 and MIS 1 (Fig. 7d; Andrews et al., 1998). 75 different paleoclimatic records from the Central Asia show moderate dry to wet climate during 40 to 30 ka (middle to late MIS 3) and dry to moderate dry condition during 21.3 to 19.8 ka (MIS 2; Table S4; Fig. 7d; Herzschuh, 2006). The strong monsoon periods observed in the above-mentioned studies are synchronous with the high rainfall phases reconstructed in this study using records from the Ganga Plain (Table S4; Figs. 7c,d).

Correlation of monsoonal rainfall with sedimentary sequences of the Indian subcontinent

Evolution of sedimentary sequences in the Ganga Plain during the Quaternary Period is linked to tectonic episodes as well as climate, especially those of glacial–interglacial cycles (Ritter et al., 1995; Kumar et al., 2007). In active orogenic belts, tectonics play considerable role on fluvial succession (DeCelles et al., 1991). On the other hand, the climatic factor controls the alluvial deposits by maintaining balance between sediment load and discharge of rivers from catchments to basin area. The change in balance causes aggradation or degradation of floodplains that can remain either attached or detached from the main channel (Gibling et al., 2005). Rainfall reconstruction for the late Quaternary from the Ganga Plain shows periodic fluctuations in rainfall during last 100 ka. These changes in rainfall could have altered the balance between sediment load and discharge rate of the rivers draining their source regions. Therefore, monsoon reconstruction based on the $\delta^{18}O$ values of soil carbonate from the Ganga Plain is compared with the sedimentary records of the Indian subcontinent.

As mentioned earlier, the IITK core is characterized by floodplain units. Sinha et al. (2007) showed that the sedimentation rate in the upper section of IITK core (1.25 mm/yr) was three times higher than that in lower section (0.4 mm/yr). The increase in sedimentation rate indicates that the amount of rainfall has increased with time. Though the rainfall record is discrete in the IITK core, the data show a sudden increase in rainfall from 36 to 31 ka, coinciding with the higher sedimentation rate. The sedimentary sequence at the bank of

https://doi.org/10.1016/j.yqres.2011.09.003 Published online by Cambridge University Press

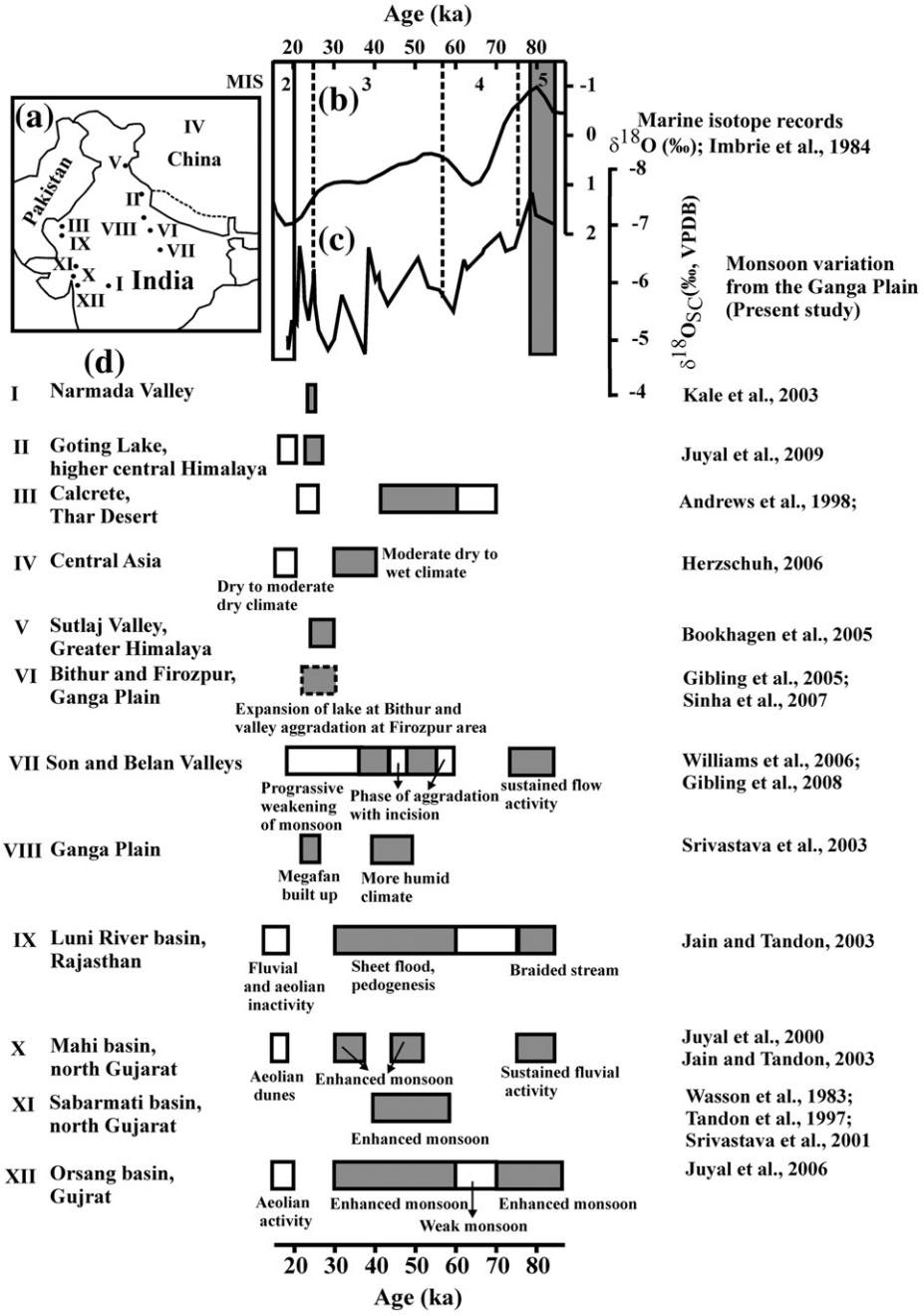

Figure 7. (a) The inset map shows spatial distribution of palaeoclimatic studies (numbers indicated refer to the records, see Fig. 7d) from different parts of the Indian subcontinent and Central Asia. (b) MIS (Imbrie et al., 1984) in relation to (c) $\delta^{18}O$ values of soil carbonate from the Kalpi core of the Ganga Plain. In MIS, overall increase in oxygen isotope ratio with time is well-correlated with the $\delta^{18}O_{sc}$ value change in the Kalpi core. A detailed comparison shows that the 84 ka monsoonal high (gray shade) and 18 ka monsoon low (white shade) are synchronous. (d) Sedimentary and geochemical records of the Indian subcontinent and Central Asia are compared with (c) monsoonal rainfall curve generated from the Ganga Plain. This comparison shows sedimentary sequences and geochemical proxies responded to high-amplitude climate changes (gray rectangles stand for high monsoon condition, white rectangles for weak monsoon and for dashed gray rectangle see section correlation of monsoonal rainfall with sedimentary sequence of the Indian subcontinent).

the Ganga River (Bithur cliff section) indicates a change from floodplain to lake deposit at around 27 ka, indicating floodplain detachment. Gibling et al. (2005) and Sinha et al. (2007) explained this detachment through incision or by change of the main channel to an underfit condition. Our data show that in the 35 to 25 ka interval, rainfall increased rapidly, suggesting detachment of floodplain through incision by the monsoon-induced high-energy river (Table S5; Figs. 7c,d; dashed gray shade block). The increasing monsoon strength from 35 to 25 ka is also evident from the aggradation phase in the Firozpur area. The reduced monsoon strength from 25 to 18 ka caused the cessation of the aggradational phase.

The sedimentary sequences of Son and Belan Valleys of the north-central India, Ganga Plain, Thar Desert (Luni River basin), margin of the Thar Desert (Mahi, Sabarmati and Orsang basin) and Narmada River of the central India show close similarities with our data (Table S5; Figs. 7a,c,d; Wasson et al., 1983; Tandon et al., 1997; Juyal et al., 2000; Srivastava et al., 2001, 2003; Jain and Tandon, 2003; Kale et al., 2003; Jain et al., 2004; Williams et al., 2006; Gibling

https://doi.org/10.1016/j.yqres.2011.09.003 Published online by Cambridge University Press

et al., 2008). Such comparison suggests that the major climatic excursions during the late Quaternary interpreted from the sedimentary sequences are broadly in phase with the monsoonal records from the Ganga Plain based on isotope geochemistry of soil profiles (Table S5; Figs. 7c,d).

Relative abundance of C_3–C_4 plants: the roles of the monsoon and atmospheric CO_2

Based on the physiological advantage of C_4 plants, Cerling et al. (1997) proposed that lower concentration of atmospheric CO_2 was the main cause of evolution and expansion of C_4 plants during the late Miocene. But the role of atmospheric CO_2 in the evolution and expansion of C_4 plants remains a matter of debate. The alkenone-based atmospheric CO_2 estimation shows rapid pCO_2 decline during Eocene/Oligocene (~33.5 Ma) boundary, much earlier than the global expansion of C_4 plants, and concentration of atmospheric CO_2 attained pre-industrial value at around 9 Ma (Pagani et al., 1999, 2005).

There is evidence of a strong influence of seasonality on the evolution of C_4 plants during the Miocene (Pagani et al., 1999; Sanyal et al., 2004, 2005, 2010). Additional attempts have been made from the late Quaternary sedimentary deposits to delineate the relative influence of atmospheric CO_2 concentration and monsoonal rainfall on the relative abundance of C_4 plants as concentration of atmospheric CO_2 is well-constrained for the late Quaternary Period (Barnola et al., 1987). Sedimentological and carbon isotope studies on the Ganga–Brahmaputra delta plain showed that the depositional environment, specifically ecological niches and climatic conditions, rather than change in atmospheric CO_2 controlled the relative abundance of C_4 plants during the LGM and Holocene (Sarkar et al., 2009). However, based on bulk organic matter and n-alkane $\delta^{13}C$ values from the Bay of Bengal sediments, Galy et al. (2008) suggested atmospheric CO_2 and humidity level together influenced the relative abundance of C_3–C_4 plants during the LGM and Holocene.

Comparison between $\delta^{18}O$ and $\delta^{13}C$ values of the Kalpi core suggests that during periods of higher rainfall C_3 plants dominated the landscape and that low-rainfall conditions are characterized by higher abundance of C_4 plants (Table S6). Overall, our data show that during the LGM local ecosystem was dominated by C_4 plants (up to 95%), whereas during times of strengthened monsoon conditions, i.e., at 25 ka, the C_4 component was reduced to about 58% (Table S6). Atmospheric pCO_2 reconstructed from the Vostok ice core for this time (28–18 ka) shows low atmospheric CO_2 levels without much variation in concentration (Barnola et al., 1987). Change in C_3–C_4 vegetational abundance without change in atmospheric CO_2 suggests a dominant role for monsoonal rainfall in the relative abundance of C_3 and C_4 plants. Also, higher abundance of C_4 plants ~30 ka when pCO_2 was high indicates a negligible effect of atmospheric CO_2 on vegetation during this time.

To check the dependency of C_3–C_4 abundance on the variation in monsoonal intensity, regression analysis between $\delta^{18}O_{SC}$–$\delta^{13}C_{SC}$ and $\delta^{18}O_{SC}$–$\delta^{13}C_{SOM}$ was done. Regression analysis between $\delta^{18}O_{SC}$–$\delta^{13}C_{SC}$ ($n=41$), and $\delta^{18}O_{SC}$–$\delta^{13}C_{SOM}$ ($n=41$) from the Kalpi core shows a statistically significant correlation ($r^2=0.20$, $p=0.002$ and $r^2=0.26$, $p=0.0003$, respectively; Figs. 8a,b), suggesting a causal relationship between the type of vegetation and rainfall. The positive slope of the plots indicates that a decrease in rainfall intensity caused an increase in the abundance of C_4 plants. Positive co-variations between $\delta^{18}Osc$ and $\delta^{13}Csc$ and absence of any relation between $\delta^{13}Csc$ and pCO_2 suggest that change in rainfall controlled the relative abundance of C_3 and C_4 plants over the Ganga Plain.

Vegetational reconstructions across the world also suggest that rainfall plays a dominant role on vegetation. A study by Huang et al. (2001) from two geographically separate lakes in the Mesoamerica shows that during the LGM, even though CO_2 concentration was low, the lake which received less rainfall was characterized by higher abundance of

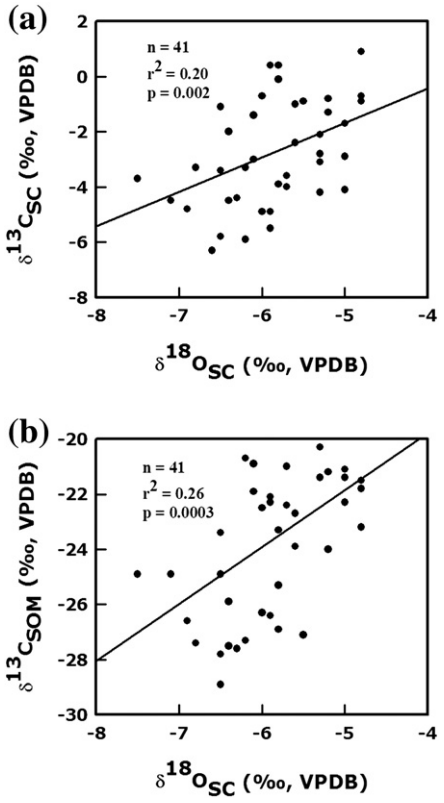

Figure 8. Regressions of (a) $\delta^{18}O_{SC}$–$\delta^{13}C_{SC}$ and (b) $\delta^{18}O_{SC}$–$\delta^{13}C_{SOM}$ shows positive correlations and indicate that decrease in rainfall intensity caused an increase in the abundance of C_4 plants.

C_4 plants. Organic carbon isotope evidence from the last glacial–interglacial loess-soil sequences shows dominant control of climate on the relative abundance of C_3 and C_4 plant in the Loess Plateau (Zhaoyan et al., 2003). $\delta^{13}C$ values of soil carbonate of the Thar Desert also show high abundance of C_3 plants before the LGM (i.e., between 25 and 60 ka) followed by high abundance of C_4 plants during the LGM (Singhvi et al., 1996; Andrews et al., 1998).

Conclusions

The Ganga Plain experienced major climatic changes in response to variation in southwest Indian monsoonal rainfall intensity during the late Quaternary Period. Monsoonal rainfall reconstruction for 100 to 18 ka shows there are three periods of monsoon intensification at about 100, 40 and 25 ka. An overall decrease of 20% in rainfall amount is observed during LGM. Vegetation during last 100 ka was characterized by mixed C_3–C_4 plants over the Ganga Plain. Increasing monsoon rainfall resulted in a higher abundance of C_3 plants and decreasing rainfall caused an increase in C_4 plants. The comparison between monsoon rainfall and atmospheric CO_2 with vegetation indicates that change in monsoonal rainfall has played a significant role in abundance variation of C_3–C_4 plants during the last 84 to 18 ka.

Acknowledgments

PS and AS gratefully acknowledge financial support from the Department of Science and Technology, New Delhi (Project No. SR/S4/ES-252/2007). PS thans Prof. Rajiv Sinha for providing the core samples. We thank two reviewers (Prof. Gregory Retallack and anonymous) and the editor, Prof. Alan Gillespie, for their critical comments and constructive suggestions which greatly benefited the paper.

https://doi.org/10.1016/j.yqres.2011.09.003 Published online by Cambridge University Press

Appendix A. Supplementary data

Supplementary data to this article can be found online at doi:10.1016/j.yqres.2011.09.003.

References

Aitken, M.J., 1998. An Introduction to Optical Dating: The Dating of Quaternary Sediments by the Use of Photon-stimulated Luminescence. Oxford University Press.

Andrews, J.E., Singhvi, A.K., Kailath, A.J., Khun, R., Dennis, P.F., Tandon, S.K., Dhir, R.P., 1998. Do stable isotope data from calcrete record late Pleistocene monsoonal climate variation in the Thar Desert of India? Quaternary Research 50, 240–251.

Auclair, M., Lamothe, M., Hout, S., 2003. Measurement of anomalous fading for feldspar IRSL using SAR. Radiation Measurements 37, 487–492.

Barnola, J.M., Raynaud, D., Korotkevich, Y.S., Lorius, C., 1987. Vostok ice core provides 160,000 year record of atmospheric CO_2. Nature 329, 408–414.

Benner, R., Fogel, M.L., Sprague, E.K., Hodson, R.E., 1987. Depletion of ^{13}C in lignin and its implications for stable isotope studies. Nature 327, 708–710.

Bhattacharya, S.K., Froehlich, K., Aggarwal, P.K., Kulkarni, K.M., 2003. Isotopic variation in Indian monsoon precipitation: records from Bombay and New Delhi. Geophysical Research Letters 30, 2285.

Bookhagen, B., Thiede, R., Strecker, M.R., 2005. Late Quaternary intensified monsoon phases control landscape evolution in the northwest Himalaya. Geology 33, 149–152.

Cane, M.A., 1998. Climate change: a role for the Tropical Pacific. Science 282, 59–61.

Cerling, T.E., 1984. The stable isotopic composition of modern soil carbonate and its relationship to climate. Earth and Planetary Science Letters 71, 229–240.

Cerling, T.E., Quade, J., Wang, Y., Bowman, J.R., 1989. Carbon isotopes in soils and palaeosols as ecology and palaeoecology indicators. Nature 34, 138–139.

Cerling, T.E., Harris, M.J., MacFadden, J.B., Leaky, G.M., Quade, J., Eisenmann, V., Ehleringer, R.J., 1997. Global vegetational change through the Miocene/Pliocene boundary. Nature 389, 153–158.

Clemens, S., Prell, W.L., 1990. Late Pleistocene variability of Arabian Sea summer monsoon winds and continental aridity: eolian records from the lithogenic component of deep sea sediments. Paleoceanography 5, 109–145.

Clemens, S.C., Prell, W.L., Murray, D., Shimmield, G., Weedon, G., 1991. Forcing mechanisms of the Indian Ocean monsoon. Nature 353, 720–725.

Clemens, S.C., Murray, D.W., Prell, W.L., 1996. Nonstationary phase of the Plio-Pleistocene Asian monsoon. Science 274, 943–948.

Clement, A.C., Seager, R., Cane, M.A., 1999. Orbital controls on the El Nino/Southern Oscillation and the tropical climate. Paleoceanography 14, 441–456.

Dansgaard, W., 1964. Stable isotope in precipitation. Tellus 16, 436–467.

DeCelles, P.G., Gray, M.B., Ridgway, K.D., Cole, R.B., Srivastava, P., Pequera, N., Pivnik, D.A., 1991. Kinematic history of a foreland uplift from Paleocene synorogenic conglomerate, Beartooth Range, Wyoming and Montana. Geological Society of America Bulletin 103, 1458–1475.

Ehleringer, J.R., 2005. The influence of atmospheric CO_2, temperature, and water on the abundance of C_3/C_4 taxa. In: Ehleringer, J.R., Cerling, T.E., Dearing, M.D. (Eds.), A History of Atmospheric CO_2 and Its Effects on Plants, Animals, and Ecosystems. Springer, pp. 214–231.

Farrera, I., Harrison, S.P., Prentice, I.C., Ramstein, G., Guiot, J., Bartlein, P.J., Bonnefille, R., Bush, M., Cramer, W., Von Grafenstein, U., Holmgren, K., Hooghiemstra, H., Hope, G., Jolly, D., Lauritzen, S.E., Ono, Y., Pinot, S., Stute, M., Yu, G., 1999. Tropical climates at the Last Glacial Maximum: a new synthesis of terrestrial palaeoclimate data, vegetation, lake-levels and geochemistry. Climate Dynamics 15, 823–856.

Feng, Z.D., Tang, L.Y., Ma, Y.Z., Zhai, Z.X., Wu, H.N., Li, F., Zou, S.B., Yang, Q.L., Wang, W.G., Derbyshire, E., Liu, K.B., 2007. Vegetation variations and associated environmental changes during marine isotope stage 3 in the western part of the Chinese Loess Plateau. Palaeogeography Palaeoclimatology Palaeoecology 246, 278–291.

Galy, V., Francois, L., France-Lanord, C., Faure, P., Kudrass, H., Palhol, F., Singh, S.K., 2008. C_4 plants decline in the Himalayan basin since the Last Glacial Maximum. Quaternary Science Reviews 27, 1396–1409.

Gibling, M.R., Tandon, S.K., Sinha, R., Jain, M., 2005. Discontinuity bounded alluvial sequences of the southern Ganga plains, India: aggradation and degradation in response to monsoonal strength. Journal of Sedimentary Research 75, 373–389.

Gibling, M.R., Sinha, R., Roy, N.G., Tandon, S.K., Jain, M., 2008. Quaternary fluvial and eolian deposits on the Belan River, India: paleoclimatic setting of Paleolithic to Neolithic archeological sites over the past 85,000 years. Quaternary Science Reviews 27, 391–410.

Goni, M.A., Ruttenberg, K.C., Eglinton, T.I., 1997. Source and contribution of terrigenous organic carbon to surface sediments in the Gulf of Mexico. Nature 389, 275–278.

Herzschuh, U., 2006. Paleo-moisture evolution in monsoonal Central Asia during the last 50,000 years. Quaternary Science Reviews 25, 163–178.

Huang, Y., Bol, R., Harkness, D.D., Ineson, P., Eglinton, G., 1996. Postglacial variations in distributions, ^{13}C and ^{14}C contents of aliphatic hydrocarbons and bulk organic matter in three types of British acid upland soils. Organic Geochemistry 24, 273–287.

Huang, Y., Street-Perrott, F.A., Perrott, R.A., Metzger, P., Eglinton, G., 1999. Glacial–interglacial environmental changes inferred from molecular and compound specific $\delta^{13}C$ analyses of sediments from Sacred Lake, Mt. Kenya. Geochimica et Cosmochimica Acta 63, 1383–1404.

Huang, Y., Street-Perrott, F.A., Metcalfe, S.E., Brenner, M., Moreland, M., Freeman, K.H., 2001. Climate change as the dominant control on glacial–interglacial variations in C_3 and C_4 plant abundance. Science 293, 1647–1651.

Huntley, D.J., Lamothe, M., 2001. Ubiquity of anomalous fading in K-feldspar and the measurement and correction for it in optical dating. Canadian Journal of Earth Sciences 38, 1093–1106.

Imbrie, J., Hays, J.D., Martinson, D.G., McIntyre, A., Mix, A.C., Morley, J.J., Pisias, N.G., Prell, W.L., Shackleton, N.J., 1984. The orbital theory of Pleistocene climate: support from a revised chronology, of the marine $\delta^{18}O$ record. In: Berger, A. (Ed.), Milankovitch and Climate, Part 1. Springer, New York, pp. 269–305.

Jain, M., Tandon, S.K., 2003. The fluvial response to the late Quaternary climate changes, western India. Quaternary Science Reviews 22, 2223–2235.

Jain, M., Tandon, S.K., Bhatt, S.C., 2004. Late Quaternary stratigraphic development in the lower Luni, Mahi and Sabarmati river basins, western India. Proceedings of the Indian Academy of Sciences — Earth and Planetary Sciences 113, 453–471.

Jain, M., Jensen, B.L., Murray, A.S., Denby, P.M., Tsukamoto, S., Gibling, M.R., 2005. Revisiting TL: dose measurement beyond the OSL range using SAR. Ancient TL 23, 9–24.

Juyal, N., Raj, R., Maurya, D.M., Chamyal, L.S., Singhvi, A.K., 2000. Chronology of late Pleistocene environmental changes in the lower Mahi basin, western India. Journal of Quaternary Science 15, 501–508.

Juyal, N., Chamyal, L.S., Bhandari, S., Bhushan, R., Singhvi, A.K., 2006. Continental record of the southwest monsoon during the last 130 ka: evidence from the southern margin of the Thar Desert, India. Quaternary Science Reviews 25, 2632–2650.

Juyal, N., Pant, R.K., Basavaiah, N., Bhushan, R., Jain, M., Saini, N.K., Yadava, M.G., Singhvi, A.K., 2009. Reconstruction of Last Glacial to early Holocene monsoon variability from relict lake sediments of the higher central Himalaya, Uttrakhand, India. Journal of Asian Earth Sciences 34, 437–449.

Kale, V.S., Mishra, S., Baker, V.R., 2003. Sedimentary records of palaeofloods in the bedrock gorges of the Tapi and Narmada rivers, central India. Current Science 84, 1072–1079.

Krull, E.S., Bestland, E.A., Gates, W.P., 2002. Soil organic matter decomposition and turnover in a tropical Ultisol: evidence from $\delta^{13}C$, $\delta^{15}N$ and geochemistry. Radiocarbon 44, 93–112.

Kumar, R., Suresh, N., Sangode, S.J., Kumaravel, V., 2007. Evolution of the Quaternary alluvial fan system in the Himalayan foreland basin: implications for tectonic and climatic decoupling. Quaternary International 159, 6–20.

Murray, A.S., Wintle, A.G., 2000. Luminescence dating of quartz using an improved single-aliquot regenerative-dose procedure. Radiation Measurements 32, 57–73.

Murray, A.S., Wintle, A.G., 2003. The single aliquot regenerative dose protocol: potential for improvements in reliability. Radiation Measurements 37, 377–381.

Nadelhoffer, K.J., Fry, B., 1988. Controls on natural nitrogen-15 and carbon-13 abundances in forest soil organic matter. Soil Science Society of America Journal 52, 1633–1640.

Osborne, C.P., Beerling, D.J., 2006. Nature's green revolution: the remarkable evolutionary rise of C_4 plants. Philosophical Transactions of the Royal Society of London. Series B, Biological Sciences 361, 173–194.

Overpeck, J., Anderson, D., Trumbore, S., Prell, W., 1996. The southwest Indian Monsoon over the last 18,000 years. Climate Dynamics 12, 213–225.

Pagani, M., Freeman, K.H., Arthur, M.A., 1999. Late Miocene atmospheric CO_2 concentrations and the expansion of C_4 grasses. Science 285, 876–879.

Pagani, M., Zachos, J.C., Freeman, K.H., Tipple, B., Bohaty, S., 2005. Marked decline in atmospheric carbon dioxide concentrations during the Paleogene. Science 309, 600–603.

Prell, W.L., Kutzbach, J.E., 1987. Monsoon variability over the past 150,000 years. Journal of Geophysical Research 92, 8411–8425.

Prell, W.L., Van Campo, E., 1986. Coherent response of Arabian Sea upwelling and pollen transport to late Quaternary monsoonal winds. Nature 323, 526–528.

Ritter, J.B., Miller, J.R., Enzel, Y., Wells, S.G., 1995. Reconciling the roles of tectonism and climate in Quaternary alluvial fan evolution. Geology 23, 245–248.

Salomons, W., Goudie, A., Mook, W.G., 1978. Isotopic composition of calcrete deposit from Europe, Africa and India. Earth Surface Process 3, 43–57.

Sangode, S.J., Bloemendal, J., 2005. Pedogenic transformation of magnetic minerals in Pliocene–Pleistocene palaeosols of the Siwalik Group, NW Himalaya, India. Palaeogeography Palaeoclimatology Palaeoecology 212, 95–118.

Sanyal, P., Bhattacharya, S.K., Kumar, R., Ghosh, S.K., Sangode, S.J., 2004. Mio-Pliocene monsoonal record from Himalayan Foreland Basin (Indian Siwalik) and its relation to vegetational change. Palaeogeography Palaeoclimatology Palaeoecology 205, 23–41.

Sanyal, P., Bhattacharya, S.K., Kumar, R., Ghosh, S.K., Sangode, S.J., 2005. Palaeovegetational reconstruction in late Miocene: a case study based on early diagenetic carbonate cement from the Indian Siwalik. Palaeogeography Palaeoclimatology Palaeoecology 228, 245–259.

Sanyal, P., Sarkar, A., Bhattacharya, S.K., Kumar, R., Ghosh, S.K., Agrawal, S., 2010. Phased intensification of monsoon, microclimate and asynchronous C4 appearance: isotopic evidence from the Indian Siwalik sediments. Palaeogeography Palaeoclimatology Palaeoecology 296, 165–173.

Sarkar, A., Ramesh, R., Somayajulu, B.L.K., Agnihotri, R., Jull, A.J.T., Burr, G.S., 2000. High resolution Holocene monsoon record from the eastern Arabian Sea. Earth and Planetary Science Letters 177, 209–218.

Sarkar, A., Sengupta, S., McArthur, J.M., Ravenscroft, P., Bera, M.K., Bhushan, R., Samanta, A., Agrawal, S., 2009. Evolution of Ganges-Brahmaputra western delta plain: clues from sedimentology and carbon isotope. Quaternary Science Reviews 28, 2564–2581.

Singh, R.L., 1994. India: A Regional Geography. National Geographical Society of India, Varanasi.

Singhvi, A.K., Banerjee, D., Ramesh, R., Rajaguru, S.N., Gogte, V., 1996. A luminescence method for dating 'dirty' pedogenic carbonates for paleoenvironmental reconstruction. Earth and Planetary Science Letters 139, 321–332.

Sinha, R., Tandon, S.K., Sanyal, P., Gibling, M.R., Stuben, D., Berner, Z., Ghazanfari, P., 2006. Calcretes from a monsoon-dominated late Quaternary interfluve in the Southern Ganga Plains: isotopic data and palaeoenvironmental implications. Palaeogeography Palaeoclimatology Palaeoecology 242, 214–239.

Sinha, R., Bhattacharjee, P., Sangode, S.J., Gibling, M.R., Tandon, S.K., Jain, M., Godfrey, D., 2007. Valley and interfluve sediments in the southern Ganga plains, India: exploring facies and magnetic signatures. Sedimentary Geology 201, 386–411.

Srivastava, P., Juyal, N., Singhvi, A.K., Wasson, R.J., Bateman, M.D., 2001. Luminescence chronology of river adjustment and incision of Quaternary sediments in the alluvial plain of the Sabarmati river, north Gujarat, India. Geomorphology 36, 217–229.

Srivastava, P., Singh, I.B., Sharma, M., Singhvi, A.K., 2003. Luminescence chronometry and late Quaternary geomorphic history of the Ganga Plain, India. Palaeogeography Palaeoclimatology Palaeoecology 197, 15–41.

Talbot, M.R., 1990. A review of the palaeohydrological interpretation of carbon and oxygen isotopic ratios in primary lacustrine carbonates. Chemical Geology 80, 261–279.

Tandon, S.K., Sareen, B.K., Someshwar Rao, M., Singhvi, A.K., 1997. Aggradation history and luminescence chronology of the Sabarmati basin, Gujarat, Western India. Palaeogeography Palaeoclimatology Palaeoecology 128, 339–357.

Wang, H., Follmer, R.L., 1998. Proxy of monsoon seasonality in carbon isotopes from paleosols of the southern Chinese Loess Plateau. Geology 26, 987–990.

Wasson, R.J., Rajaguru, S.N., Misra, V.N., Agrawal, D.P., Dhir, R.P., Singhvi, A.K., Rao, K.K., 1983. Geomorphology, late Quaternary stratigraphy and paleoclimatology of the Thar dune field. Zeitschrift für Geomorphologie 45, 117–151.

Wedin, D.A., Tieszen, L.L., Dewey, B., Pastor, J., 1995. Carbon isotope dynamics during grass decomposition and soil organic matter formation. Ecology 76, 1383–1392.

Williams, M.A.J., Pal, J.N., Jaiswal, M., Singhvi, A.K., 2006. River response to Quaternary climatic fluctuations: evidence from the Son and Belan valleys, north-central India. Quaternary Science Reviews 25, 2619–2631.

Wright, J.D., 2000. Global Climate Change in Marine Stable Isotope Records. American Geophysical Union.

Wynn, J.G., Bird, M.I., 2007. C_4-derived soil organic carbon decomposes faster than its C_3 counterpart. Global Change Biology 13, 2206–2217.

Yurtsever, Y., Gat, J.R., 1981. Atmospheric waters. In stable isotope hydrology: deuterium and oxygen-18 in the water cycle. Technical Report Series, IAEA, Vienna, 210, pp. 103–142.

Zhaoyan, G., Qiang, L., Bing, X., Jiamao, H., Shiling, Y., Zhongli, D., Tungsheng, L., 2003. Climate as the dominant control on C3 and C4 plant abundance in the Loess Plateau: organic carbon isotope evidence from the last glacial–interglacial loess-soil sequences. Chinese Science Bulletin 48, 1271–1276.

https://doi.org/10.1016/j.yqres.2011.09.003 Published online by Cambridge University Press